Submitted: 10 August, 2022 Accepted: 29 November, 2022 Published: 15 August, 2023 DOI:10.22514/ejgo.2023.058

ORIGINAL RESEARCH

European Journal of Gynaecological Oncology

PI3K inhibitor promotes tumor vessel normalization and improves treatment outcomes of breast cancer with doxorubicin

Baihui Li[1,†], Yuanyuan Tian[1,†], Ju Huang[1], Haiying Zhang[1], Jiao Zhao[1], Lihong Zhang[1], Wei Li[1,*]

[1]The Key Laboratory of Pathobiology, Ministry of Education, The College of Basic Medical Sciences, Jilin University, 130021 Changchun, Jilin, China

***Correspondence**
liwei2006@jlu.edu.cn
(Wei Li)

[†] These authors contributed equally.

Abstract

HS-173 is a specific inhibitor of the Phosphoinositide 3-Kinase α (PI3Kα) subtype. Although it was shown to potentially inhibit tumor angiogenesis, experimental validation studies are still needed. This study provides an experimental basis for the role of HS-173 in breast cancer. A mouse model of subcutaneous transplantation breast cancer was constructed. The mice were treated with different concentrations of HS-173. Immunohistochemical staining was used to detect tumor microvessel density, and the appropriate concentration was determined. Immunofluorescence was used to detect the morphology integrity of tumor vessels' lumen, transmission electron microscopy to detect tight junctions between endothelial cells and the integrity of the basement membrane, Doppler ultrasound to detect tumor blood perfusion, and small animal live imaging to detect the penetration of doxorubicin in the tumor tissues. After HS-173 treatment, the number of tumor interstitial microvessels decreased, the lack of tumor vascular lumen was reduced, and the continuity and integrity of the vascular lumen were increased. Vascular endothelial cells showed complete morphology with good tight junctions. The extracellular matrix was rich in components and tended to form basement membranes. HS-173 also increased the blood perfusion in the tumor tissue compared with the doxorubicin treatment alone. Further, the fluorescence signal intensity of the tumor tissue doxorubicin was significantly enhanced after HS-173 treatment. The PI3K inhibitor HS-173 showed promising potential in inhibiting tumor angiogenesis and improving the structure and function of blood vessels in the tumor microenvironment.

Keywords

Tumor blood vessels; Normalization of tumor blood vessels; PI3K inhibitors; Breast cancer

1. Introduction

In 2020, there were an estimated 19.3 million new cancer cases and nearly 10 million cancer deaths worldwide, according to estimates of global cancer incidence and mortality published by the International Agency for Research on Cancer. Among them, female breast cancer surpassed lung cancer as the most common tumor, with an estimated nearly 2.3 million new breast cancer cases (11.7%) and 685,000 deaths, ranking fifth in cancer-related deaths worldwide. Traditional anti-cancer therapy, such as chemotherapy, radiotherapy, endocrine therapy, targeted therapy and others, mainly achieve therapeutic purpose by inhibiting the proliferation of tumor cells.

However, due to the abnormal formation of tumor blood vessels, tumor cells can still obtain a continuous supply of oxygen and nutrients and continue to grow. At the same time, it is difficult for traditional drugs and immune cells to penetrate the abnormal tumor blood vessels, resulting in drug resistance and making antitumor therapy challenging, thus prompting researchers to start investigating new perspectives on antitumor therapy.

Tumor blood vessels are channels for malignant tumors to provide nutrients and implement metastasis. To allow tumor tissues to meet their blood supply demand for their excessive proliferation, tumor cells secrete a large number of pro-angiogenic factors to promote angiogenesis [1]. However, due to the large secretion of pro-angiogenic factors and excessive consumption of anti-angiogenic factors, the new blood vessels may not attain maturity or may even show abnormalities [2], including tortuous and swollen morphology, luminal intussusception, thinning or missing of the tube wall, loose connections between vascular endothelial cells, lack of pericyte coverage, and incomplete basement membrane [3]. These abnormalities in morphology and structure increase the permeability of tumor vessel walls and decrease vascular perfusion, leading to severe ischemia, hypoxia and acidosis in tumor tissues. Further, these abnormalities in blood vessels and the microenvironment hinder the delivery of cytotoxic drugs to tumoral tissues, leading

to varied antitumor effects [4–7].

In recent years, it was found that PI3K inhibitors such as BEZ-235 (Dactolisib) and BKM120 (Buparlisib) could inhibit tumor neogenesis and promote the normalization of blood vessels to increase the radiotherapy effects. However, these PI3K inhibitors are the overall inhibitors of PI3K and its downstream mTOR (mammalian target of rapamycin) signaling pathway or the common inhibitors of all types of PI3K, and it remains unclear whether they have any effect on the proliferation of normal cells. HS-173, a specific inhibitor of the PI3Kα subtype, can selectively inhibit the PI3Kα subtype involved in regulating tumor angiogenesis. Previous studies confirmed that HS-173 inhibited the proliferation of pancreatic cancer cells and the migration and epithelial-mesenchymal transition mediated by TGF-β. Park *et al.* [8], eported that the inhibition of the PI3K/AKT (protein kinase B, PKB) pathway by HS-173 significantly radiosensitized pancreatic cancer to subsequent radiation effects, as demonstrated by an increase in apoptosis and altered cell cycle resulting from the inhibition of DNA repair response. A recent study by Park *et al.* [8] revealed that HS-173 inhibited the proliferation of radiation-resistant triple-negative breast cancer MDA-MB-231 cells and induced G2/M arrest, in addition to apoptosis by inhibiting the PI3K/AKT pathway, particularly when combined with radiation treatment. Other researchers have also proved that HS-173 could promote tumor cell apoptosis and inhibit angiogenesis. However, the promoting effects of HS-173 on tumor angiogenesis and vascular normalization are yet to be fully clarified.

PI3K and its downstream signaling molecules have recently been discovered to have important effects on the blood vessels, lymphatic vessels and immune cells in the tumor stroma. The PI3Kα subtype is mainly involved in maintaining the stability of endothelial cells and angiogenesis. To clarify the effects of PI3Kα subtype inhibitors on tumor angiogenesis, vascular structural integrity and chemotherapeutic drug delivery function, we used HS-173, a PI3Kα subtype-specific inhibitor, and broad-spectrum chemotherapeutic drug doxorubicin (DOX) for single or combined treatment.

Small animal ultrasound was used to monitor the growth status of the subcutaneous xenograft tumor model after inoculation with 4T1, a mouse breast cancer cell line. HE (Hematoxylin-eosin) staining, immunohistochemical staining, immunofluorescence staining and transmission electron microscopy respectively showed that HS-173 could inhibit angiogenesis, reduce the tortuosity, expansion and structural disorder of tumor blood vessels, increase the integrity of tumor vascular endothelium, and enhance the tight junctions between endothelial cells and basement membrane integrity. Doppler ultrasound and *in vivo* imaging showed that HS-173 increased the blood perfusion and delivery of doxorubicin in tumor tissues. Based on the observed tumor volume after the combined treatment, we found that HS-173 enhanced the treatment effects of doxorubicin.

Overall, this experimental study concluded that HS-173 could inhibit tumor angiogenesis, promote the normalization of tumor vascular structure and function, and increase the therapeutic effects of chemotherapy drugs, providing experimental evidence for further tumor vascular normalization research.

2. Material and methods

2.1 Animals and cell culture

This study used 6–8 week old female BALB/C mice weighing 18–20 g. The experimental animals were kept in the animal room of Jilin University School of Basic Medicine and were provided by Beijing Huafukang Biotechnology Co., Ltd. (license number: SCXK (Ji) 2018-0001). The cell line used in this study was 4T1, a mouse breast cancer cell line provided by the Department of Pathology, Jilin University School of Basic Medicine. The 4T1 cells were grown in RPMI (Roswell Park Memorial Institute) 640 Medium (GIBCO) containing 10% fetal bovine serum (MRC) at 37 °C and 5% CO_2.

2.2 Drugs and reagents

The drugs used in this experiment were PI3Kα subtype-specific inhibitor (HS-173) and broad-spectrum chemotherapeutic drug Doxorubicin, both purchased from Selleck (the United States). CD31 antibody was purchased from Abcam; Goat anti-rabbit IgG-FITC was purchased from Bioworld. Goat serum was purchased from Solarbio. DMSO was purchased from Sigma. The immunohistochemistry kit and DAB color developing fluid were purchased from Fuzhou Maixin Biotech.

2.3 Experimental design

A total of 20 female BALB/C mice aged 6–8 weeks were obtained, and each mouse was subcutaneously injected with 5 $\times$ 10^5 4T1 cells in 100 μL of PBS (phosphate buffer solution) to establish a subcutaneously transplanted breast cancer model. After inoculation, the skin condition of the mice was observed to judge the tumor formation. The mice were randomly divided into the following four study groups, with five mice in each group: A solvent control group (control group), treated with 5% DMSO (Dimethyl sulfoxide) + PEG (Polyethylene glycol) 400 + 35% ddH_2O (double distilled H_2O); HS-173 alone administration group (HS-173 group), treated with two concentrations of HS-173; the 30 mg/kg group, which used a 6 mg/mL solvent-prepared working solution at a dose of 0.1 mL/only, and; the 10 mg/kg group, which used a solvent-prepared working solution concentration of 2 mg/mL at a dose of 0.1 mL/only. The doxorubicin alone administration group (DOX group) was treated with doxorubicin 5 mg/kg, using a working solution prepared with solvent at a concentration of 1 mg/mL and dose 0.1 ml/only. The HS-173 and adriamycin combination group (H + D group) was treated similarly to the HS-173 group, in addition to administering 5 mg/kg doxorubicin. The administration started when the transplanted tumor volume grew to 50 mm^3. The intraperitoneal injection was administered once every 2 days until the 20th day after the tumor was implanted for a total of 6 administrations. After the end of the administration, the tumor in each mouse was harvested for immunohistochemistry (IHC). The lung, liver and kidney tissues of each group of mice were separated for HE staining.

2.4 Small animal ultrasound

The mice underwent an ultrasound every 3 days after the start of the administration to monitor the growth of the mouse breast cancer xenografts. They were anesthetized with 0.8% sodium pentobarbital intraperitoneal injection, their hair was removed at the tumor site, and the mice were fixed on the operating table. Using an ultrasound coupling agent at the tumor site, we observed the echo intensity and range of the tumor site in the ultrasound mode, determined the condition and size of the lesion, and the same operator performed image acquisition and measurement for each inspection.

2.5 Hematoxylin-Eosin (HE) staining, Immunohistochemistry (IHC) staining and immunofluorescence

The formalin-fixed breast tissues were embedded in paraffin blocks. Sliced sections (2 μm) were deparaffinized and rehydrated by a xyleneethanol-water gradient system. Then, HE staining was performed, followed by a dehydrating process.

IHC staining was performed using an IHC kit (Fuzhou Maixin Biotech). Briefly, after deparaffinization and rehydration, 4T1 tumor tissue paraffin sections (2 μm) were subjected to heat-induced epitope retrieval using EDTA (EthyleneDiamine Tetraacetic Acid). Then, the sections were treated with a blocking buffer and subsequently incubated overnight (at 4 °C) with primary Abs against CD31—1:100 dilution. Next, the sections were incubated with HRP (Horseradish peroxidase)-conjugated secondary Abs and diaminobenzidine was used to visualize the immunoreaction. The nuclei were counterstained with hematoxylin, and IHC-staining images were captured using a microscope (OLYMPUS).

The tumor microvessel density counting method was performed as follows. First, we selected CD31 positive sites under a low-power field of view. Then, we counted a single brown-yellow endothelial cell or a lumen surrounded by multiple endothelial cells under a high-power microscope. However, it should be noted that vessels with a lumen diameter greater than the diameter of 8 red blood cells were not listed in the count range.

For immunofluorescence labeling, BMDMs (Bone marrow derived macrophage) were washed with PBS, fixed with 4% formaldehyde, blocked with 10% goat serum for 1 h at room temperature, and incubated overnight (at 4 °C) with a primary antibody (CD31—1:100). Then, the cells were washed, incubated with fluorescently labeled secondary antibody (goat anti-mouse 1:300), followed by incubation at room temperature for 1 h. Next, the secondary antibody was washed off, the nucleus was stained with DAPI (4′, 6-diamidino-2-phenylindole) for 5–8 min at room temperature, then after the DAPI staining solution was washed, the slide was mounted with an anti-fluorescence quencher and examined using a fluorescence microscope.

2.6 TEM (Transmission Electron Microscope) sample preparation

The mice were sacrificed, the tumor tissue was stripped, and fresh tissue pieces were cut into 1 mm^3 square and soaked in glutaraldehyde at 4 °C for 24 h. After rinsing with PBS, they were soaked in 2% osmium acid and fixed at 4 °C for 24 h. After dehydration with 50%, 70%, 90% and 100% acetone, they were left for 10 min each for three times. Then, benzidine disulfonic acid, methyl methacrylate, epoxy resin 812 and DMP-30 were mixed to form an embedding agent and embedded at 60 °C for 24 h. The tissue block was assessed under a dissecting microscope to determine the position of the slice. Using a microtome to semi-thinly section the surface to be observed, the slide was stained with toluidine blue, and the observation field was selected under a microscope. Next, an ultra-thin microtome was used to make ultra-thin sections of the selected field of view, double stained with uranyl acetate and lead nitrate, and they were observed with a transmission electron microscope.

2.7 Live imaging of animals

First, doxorubicin was diluted to 1/100 of the body concentration and added to a 96-well plate. The optimal wavelengths for the emission/absorption of doxorubicin were determined to be 500/600 and 500/620. Then, 5 mg/kg of adriamycin was injected into the tail vein 24 h before imaging. A depilatory cream was used to remove the hair at the tumor site during the operation, following which the mice were anesthetized with 0.8% sodium pentobarbital, and the fluorescence intensity of adriamycin was detected. After the *in vivo* experiment, the tumor tissue was removed and placed in a clean petri dish to detect the fluorescence intensity of adriamycin in tumor tissue.

2.8 Statistical processing

Data were analyzed with the SPSS 22.0 software (IBM Corporation, Armonk, NY, USA). Quantitative data were analyzed using either *t*-tests (for two groups) or one-way ANOVA (Analysis of Variance) (for multiple groups). All experiments were repeated at least thrice, and the corresponding data are shown as mean ± SEM (Structural equation modeling). * represented $p < 0.05$ and ** represented $p < 0.01$, which indicated a significant statistical difference.

3. Result

3.1 Establishment of subcutaneous transplanted tumor tissue of mouse breast cancer and detection of its growth status

The mouse breast cancer cell line 4T1 was cultivated and inoculated on the back of female BABL/C mice. Then, the health of the mice and the growth of subcutaneous transplanted tumors after inoculation were observed. The formation of solid tumors could be seen by the naked eyes, which showed the tumors to demonstrate nodular or lobulated morphology, with a fiber envelope around them (Fig. 1A). The tumor-bearing mice were randomly divided into 3 groups (5 mice/group), were given the same dose of solvent, low-dose HS-173 (10 mg/kg) and high-dose HS-173 (30 mg/kg), and therapeutic research on each group of mice were conducted (one mouse died in the control group). The tumor volume changes were measured with a vernier caliper every day after the treatment

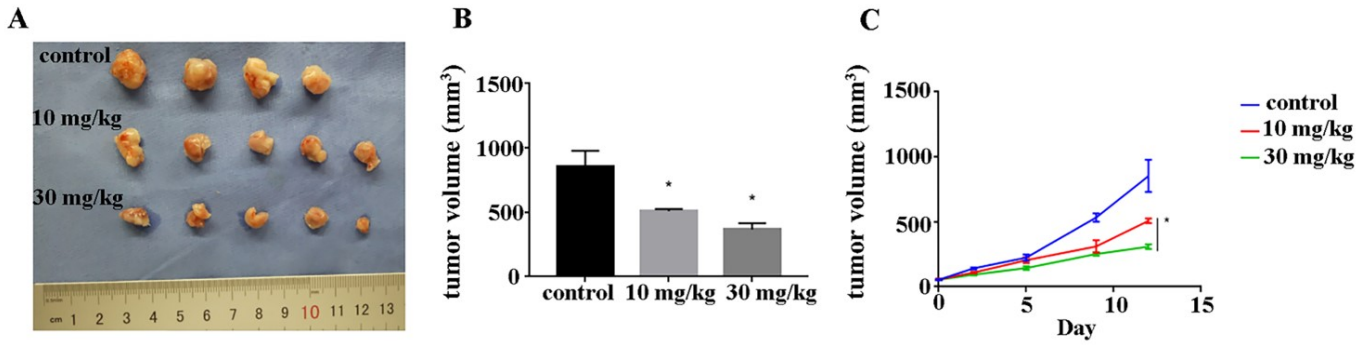

FIGURE 1. Breast cancer tissue after HS-173 treatment. (A) General view of breast cancer tissue after HS-173 treatment. The tumor-bearing mice were randomly divided into 3 groups, 5 in each group, and were given the same dose of solvent, low-dose HS-173 (10 mg/kg) and high-dose HS-173 (30 mg/kg). One mouse died in the control group. The tumor volume changes were measured using a vernier caliper every day after the administration. (B) After HS-173 treatment, the tumor volume increased more slowly than in the control group. The tumor volume of the mice in the low-dose and high-dose HS-173 administration group was significantly smaller than in the control group (*$p < 0.05$). (C) Statistical graph of tumor volume change after 12 days of treatment revealed that the rate of tumor volume increase in the low-dose and high-dose administration groups was decreased compared with the control group (*$p < 0.05$).

administration. At the end of the administration, the lungs, liver and kidneys of each group of mice were taken for HE staining. The results showed that after HS-173 treatment, the tumor volume increased slower than in the control group. After treatment, the tumor volume of the mice in the low-dose and high-dose HS-173 administration group was statistically smaller than that of the control group ($p < 0.05$) (Fig. 1B). During the administration process, compared with the control group, the rate of tumor volume increase in the low-dose and high-dose administration groups decreased (Fig. 1C). The HE staining results of the liver, kidney and lung tissues of the mice in each group showed that the liver, kidney and lung tissues of the mice in the different administration groups were intact and had no tumor metastasis (Fig. 2).

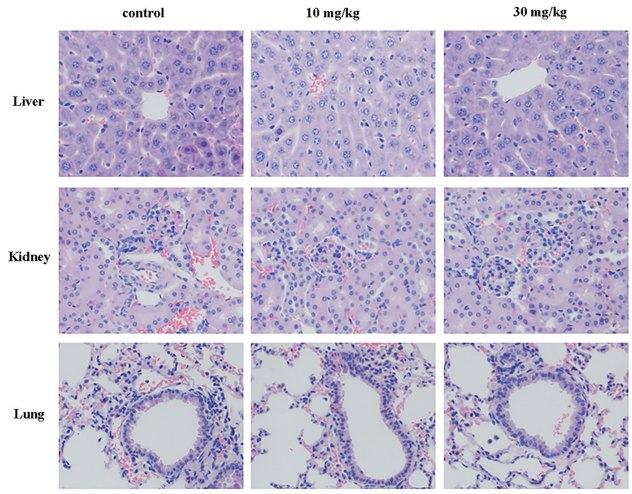

FIGURE 2. HE staining images of the main organs in each group after treatment (200×). The HE staining results of the liver, kidney and lung tissues of mice from each group showed that the corresponding tissues of the mice in the different administration groups were intact, and no tumor metastasis was found.

3.2 Detection of the number of new blood vessels in breast cancer tissue

To explore the promoting effects of HS-173 on the "normalization of blood vessels" of tumors, it was necessary to detect whether tumor tissue angiogenesis was inhibited. First, the mice were taken 12 days after the administration, the tumor tissues were stripped, and paraffin sections were prepared. Second, immunohistochemical staining was used to detect the expression of vascular endothelial cell marker CD31. The results showed that compared with the control group, the number of microvessels in the tumor tissues tended to decrease after HS-173 administration (Fig. 3A–C). After counting the microvessel density MVD (microvessel density) of each group, we found that the MVD of tumor tissues was reduced after HS-173 administration at different doses (10 mg/kg and 30 mg/kg) compared with the control group (Fig. 3D). There was a statistical difference between the 10 mg/kg administration group and the control group ($p < 0.05$). In addition, the 30 mg/kg HS-173 administration group was significantly different from the control group ($p < 0.01$).

3.3 Animal ultrasound detection of tumor volume after a single application of doxorubicin and its combination with PI3K treatment

The tumor-bearing mice were randomly divided into 4 groups and were given solvent, adriamycin, HS-173 and adriamycin combined with HS-173 intraperitoneally for 12 days. After the treatment, the tumor volume of each group was detected by a small animal ultrasound instrument. The results showed that after treatment with doxorubicin alone or HS-173 alone, the tumor volume was smaller than the control group ($p < 0.05$) (Fig. 4A). In addition, the tumor volume of the combined drug group was significantly smaller than the single drug group ($p < 0.01$) (Fig. 4B).

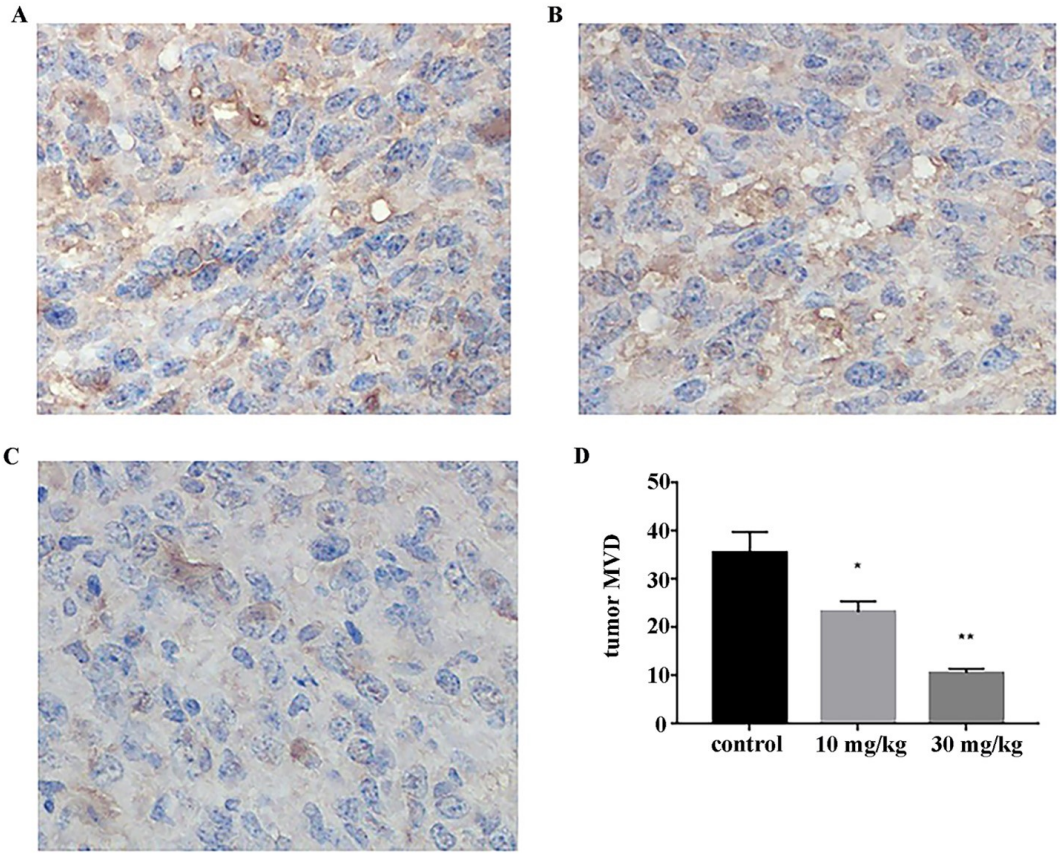

FIGURE 3. CD31 expression in each group by immunohistochemical staining (400×). (A) Control group (B) 10 mg/kg group (C) 30 mg/kg group (D) MVD statistics of tissues (*$p < 0.05$, **$p < 0.01$). Compared with the control group, the number of microvessels in tumor tissues tended to decrease after HS-173 administration. There was a statistical difference between the 10 mg/kg administration group and the control group (*$p < 0.05$), and the 30 mg/kg HS-173 administration group was significantly different from the control group (**$p < 0.01$).

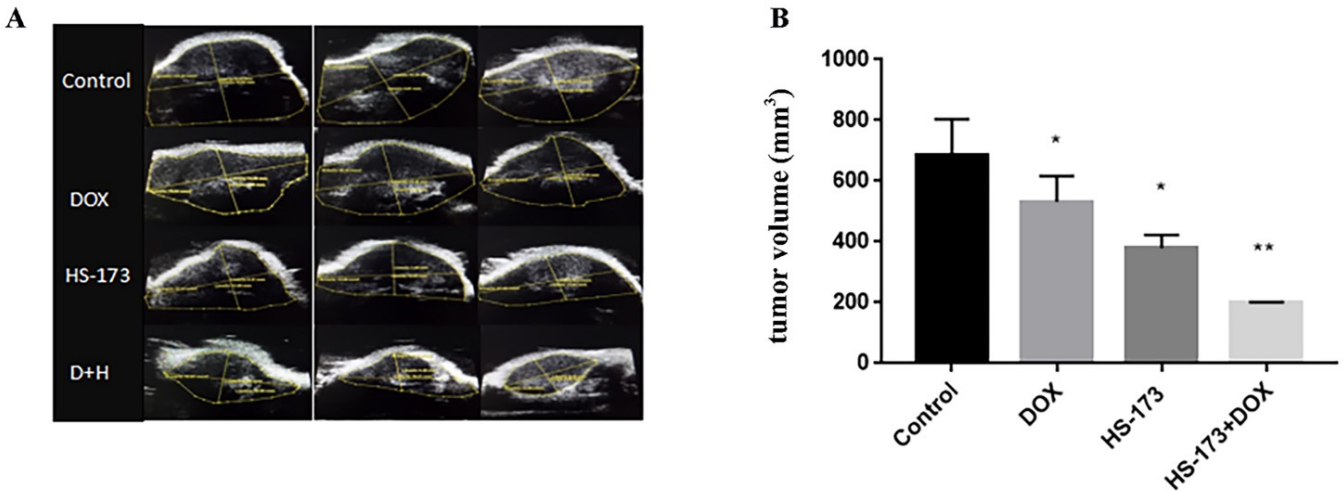

FIGURE 4. Ultrasound examination results of each group of tumors after treatment. (A) The tumor-bearing mice were randomly divided into 4 groups and were given solvent, adriamycin, HS-173 and adriamycin combined with HS-173 intraperitoneally for 12 days. After the treatment, the tumor volume of each group was detected by a small animal ultrasound instrument. (B) The results showed that after treatment with doxorubicin alone or HS-173 alone, the tumor volume was smaller than the control group (*$p < 0.05$). In addition, the tumor volume of the combined drug group was significantly smaller than the single drug group (**$p < 0.01$). DOX: doxorubicin; HS-173: PI3Kα subtype-specific inhibitor; D + H: adriamycin combination group.

3.4 Immunofluorescence staining to detect the distribution and integrity of vascular endothelial cells

We selected 30 mg/kg HS-173 as the dose for subsequent experiments based on previous experimental observations. The mice were inoculated according to the above-mentioned subcutaneous transplantation tumor inoculation method. After tumor formation, the mice were randomly divided into 4 groups, with 5 mice in each group. The average tumor volume was the same as the average weight of the mice, and the same dose of solvent, doxorubicin (DOX), HS-173 and the combination of doxorubicin and HS-173 were administered to each group of mice for therapeutic research. To further explore the effects of HS-173 on tumor vascular structure, we made paraffin sections of tumor tissues from 4 groups of mice treated with different administrations. Immunofluorescence staining was used to detect the vascular endothelial cell marker CD31 and the continuity and integrity of tumor vascular endothelium in each group of tumor-bearing mice. The results showed that the control and adriamycin groups had different degrees of vascular endothelium loss, the vascular lumen was discontinuous, and the integrity was reduced. The HS-173 group and the combination group had better endothelial cell integrity and continuity (Fig. 5).

3.5 Transmission electron microscopy to observe the integrity of vascular endothelial cell tight junctions and basement membrane

To explore the effects of HS-173 on the structural integrity of tumor blood vessels, we used transmission electron microscopy to observe the tight junctions between the tumor vascular endothelial cells and integrity of vascular basement membrane in the control group, adriamycin group, HS-173 group, and the combination medication group. The results are shown in Fig. 6. Under the electron microscope, the blood vessels in the interstitial tissue of the tumor tissues demonstrated luminal-like structures, which were mostly surrounded by one or two endothelial cells and red blood cells (R) in the middle of part of the lumens. In the control group, the vascular lumens of tumor tissues were enlarged and twisted. The endothelial cells showed abnormal morphology and incomplete structure, with poor tight junctions between the endothelial cells. The extracellular matrix components were fewer, and no basement membrane was formed. The tumor vessel lumen in the doxorubicin administration group was incomplete or missing, and its characteristics were similar to those in the control group. In the HS-173 administration and the combination medication groups, the tumor vascular lumens were relatively regular, the endothelial cell structure was complete, the connection between the endothelial cells was tight, and the number was large. In addition, their extracellular matrix was rich in components and tended to form a basement membrane.

3.6 Color Doppler ultrasound dynamic monitoring of tumor vascular perfusion

The perfusion of blood vessels represents its delivery function, and the performance of cytotoxic drugs depends on the delivery function of blood vessels. The small animal ultrasound system used in this experiment had its own color Doppler mode. In this mode, the blood flow in the tissue was marked by red and blue color signals, representing the blood flow signal in the opposite direction. It also detected the current local blood perfusion volume and location distribution of the tumor over time. In this experiment, ultrasound images at different time points in the same time period were selected for each group of mice. The average blood flow signal area in the tumor tissue of each group of mice was calculated to compare the blood perfusion volume of each group. As shown in Fig. 7A–D the results indicated that the blood perfusion volume of tumor tissue in the HS-173 administration group and the combination medication group was significantly higher than in the solvent control group and the adriamycin administration group. In the control group and the DOX treatment group alone, the tumor blood perfusion only appeared around the tumor and did not enter the tumor tissues. After HS-173 treatment, we observed varying degrees of increasing blood perfusion trends in the tumor tissue (Fig. 7E).

3.7 Application of small animal live imaging to detect the delivery of doxorubicin in tumor tissues

Doxorubicin is a broad-spectrum chemotherapeutic drug with its own fluorescent signal, which can show red fluorescence under a certain wavelength of excitation light source. After pre-experimental testing, we selected two groups of doxorubicin optimal excitation/absorption wavelengths as 500/600 nm and 500/620 nm. Afterward, a small animal live imaging device was used to detect the fluorescence signal intensity of doxorubicin in the tumor tissue in the optimal wavelength range to obtain the delivery amount of doxorubicin in the tumor tissue. The result showed that compared with the treatment with doxorubicin alone, the fluorescence signal of doxorubicin in the tumor tissue was stronger after HS-173 treatment (Fig. 8A). Statistical analysis of the measured ROI (region of interest) of doxorubicin in the tumor tissues indicated that the results were statistically significant ($p < 0.01$) (Fig. 8B). Altogether, these findings show that HS-173 could increase the delivery efficiency of doxorubicin in tumor tissues.

4. Discussion

Breast cancer is currently the most serious malignant tumor threatening women's health and is ranked first in the incidence of female malignant tumors. It greatly threatens women's health, especially when it has metastasized. Although different treatments such as chemotherapy, endocrine therapy and targeted therapy are used to control the pathogenesis of breast cancer more effectively, breast cancer metastasis and recurrence still account for a large number of cancer-related deaths [7]. Angiogenesis is an important process for tumor growth and proliferation. The new blood vessels provide channels

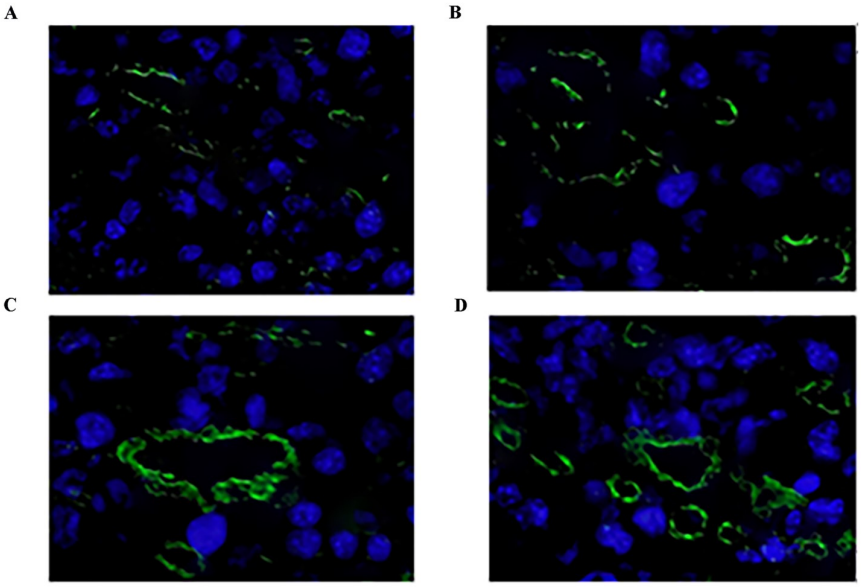

FIGURE 5. CD31 immunofluorescence expression in each group (400×). (A) Control group (B) DOX group (C) HS-173 group (D) H + D group Immunofluorescence staining was used to detect the vascular endothelial cell marker CD31 and to detect the continuity and integrity of tumor vascular endothelium in each group of tumor-bearing mice. The results showed that the (A) control group and (B) adriamycin group had different degrees of vascular endothelium loss, and the vascular lumen was discontinuous, and the integrity was reduced; (C) the HS-173 group and (D) combination group had better endothelial cell integrity and continuity.

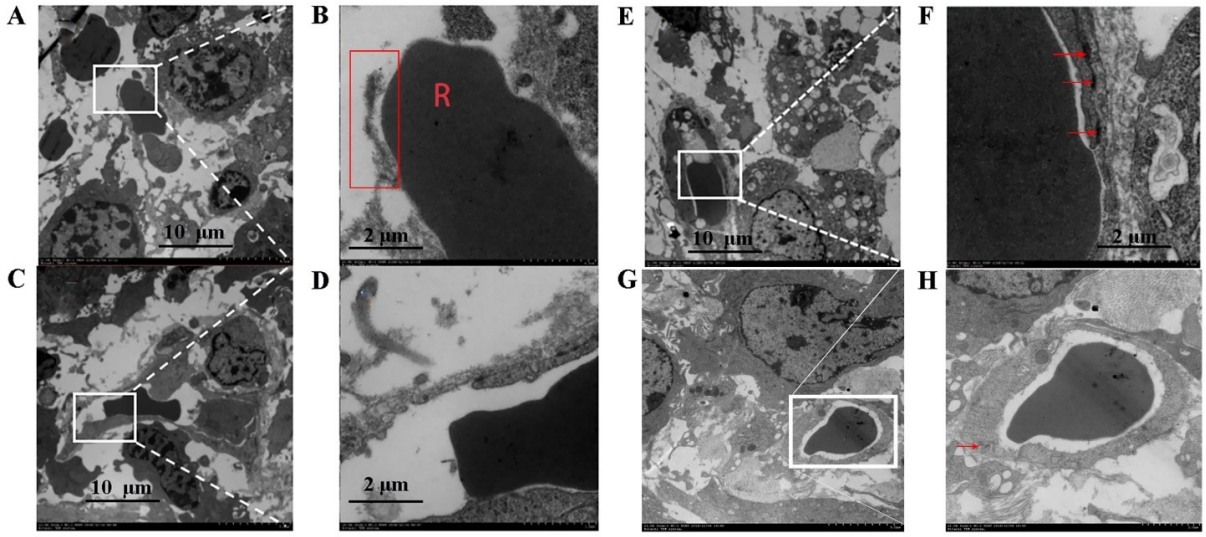

FIGURE 6. Transmission electron microscopy to observe the changes in blood vessel structure in each group (A, C, E, G: ×1000; B, D, F, H: ×5000). (A) Control group, (C) DOX group, (E) HS-173 group, and (G) H + D group under electron microscopy. The blood vessels in the interstitial tissue of the tumor tissues demonstrated luminal-like structures, mostly surrounded by one or two endothelial cells and red blood cells (R) in the middle of part of the lumens. (A, B) In the control group, the vascular lumens of tumor tissues were enlarged and twisted. Endothelial cells had abnormal morphology, incomplete structure and poor tight junctions between endothelial cells. Extracellular matrix components were fewer, and no basement membrane was formed. (C, D) The tumor vessel lumen in the doxorubicin administration group was incomplete or even missing, and its characteristics were similar to those in the control group. (G, H) In the HS-173 administration group and the combination medication group, the tumor vascular lumens were relatively regular, the endothelial cell structure was complete, the connection between the endothelial cells was tight, and the number was large. The extracellular matrix was rich in components, and there was a tendency to form a basement membrane.

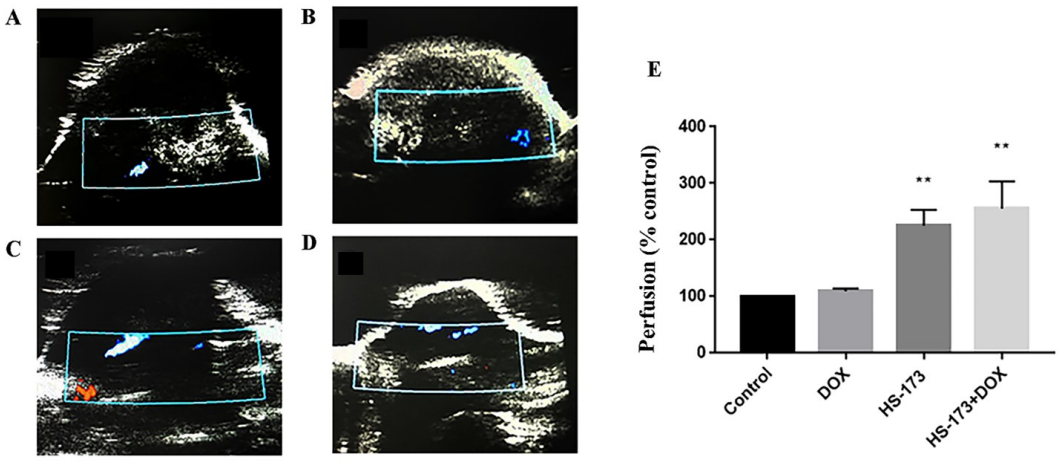

FIGURE 7. Doppler ultrasound detection of blood flow changes in each group after treatment. (A) Control group, (B) DOX group, (C) HS-173 group, (D) H + D group, and (E) statistics chart of blood perfusion of tumor tissue (**$p < 0.01$). The blood perfusion volume of tumor tissue in the HS-173 administration group and the combination treatment group was significantly higher than the solvent control group and the adriamycin administration group. In the control group and the DOX treatment group alone, the tumor blood perfusion only appeared around the tumor and did not enter the tumor tissue. After using HS-173 treatment, we observed varying degrees of increasing blood perfusion trends in the tumor tissue. DOX: doxorubicin; HS-173: PI3Kα subtype-specific inhibitor.

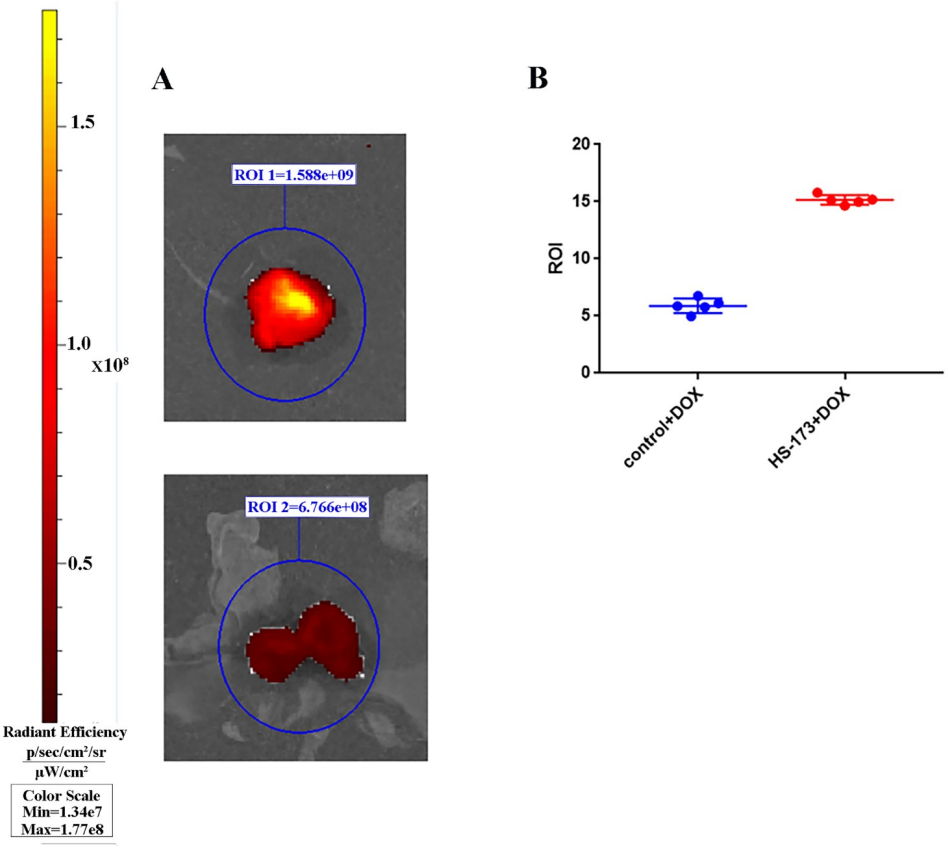

FIGURE 8. Fluorescence signal intensity of adriamycin in tumor tissues. (A) Fluorescence signal intensity map of adriamycin in tumor tissues. (B) Statistic graph of fluorescence intensity of doxorubicin in tumor tissue (**$p < 0.01$) compared with the treatment with doxorubicin alone, the fluorescence signal of doxorubicin in the tumor tissue is stronger after HS-173 treatment. We conducted statistics on the measured ROI of doxorubicin in tumor tissues and found that the results were statistically significant (**$p < 0.01$). It shows that HS-173 could increase the delivery efficiency of doxorubicin in tumor tissues. DOX: doxorubicin; HS-173: PI3Kα subtype-specific inhibitor; ROI: region of interest.

for tumor cells and participate in the formation of abnormal microenvironments such as hypoxia and acidosis, which affect the therapeutic effects of cytotoxic drugs [9, 10]. However, simply inhibiting tumor angiogenesis has been shown insufficient in curbing the development of tumors. Jain *et al.* [11] reported that angiogenesis inhibitors could moderately inhibit angiogenesis, "normalize" tumor blood vessels and restore the structure and function of blood vessels. In addition, it can provide suitable treatment time and dose reference for other cytotoxic treatments [11, 12].

The mouse breast cancer 4T1 cell line used in this experiment is a highly metastatic breast cancer cell line which is originated from BABL/C mice; thus, it can avoid immune rejection caused by human tumor cells. It also has low allograft immunogenicity and a high tumor formation rate. The tumor formation rate is 100% as measured by preliminary experiments, which provides a good experimental animal model for follow-up research. In this study, we used light microscopy to observe the breast cancer tissues of transplanted tumor mice, which showed that the tumor cells proliferated rapidly and new blood vessels were abundant. The blood vessels in the tumor stroma were mostly immature blood vessels with abnormal structure and function. The tube wall was tortuous and irregular, endothelial cells were loosely connected, tumor cells and red blood cells could be seen in the tube cavity, and a tube-like structure surrounded by suspected tumor cells could be seen. In this experiment, color Doppler ultrasonography was used to dynamically observe the blood perfusion in the tumor tissues of living mice. The testing instrument used was a small animal high-frequency ultrasound system. The operation method was to fix the mouse under the ultrasound probe and collect the contrast image of the tumor site with the ultrasound coupling agent. Therefore, the subcutaneous vaccination method used in this experiment could avoid the blood flow interference signal generated by the chest cavity and the large blood vessels of the abdomen that may be caused by *in situ* vaccination. In addition, the blood perfusion of the tumor tissues was more clearly observed. We visually and accurately monitored tumor growth images 3 days after inoculation. The tumor tissue recognition was high, the image was clear, the lesion area could be observed, the operation was simple, and special consideration was taken to reduce animal suffering. Overall, the images represent reliable data for monitoring tumor volume changes.

A tumor is a complex organ-like structure. Compared with normal tissues, tumor cells need more blood vessels to transport oxygen and nutrients to maintain their rapid proliferation needs. Tumor tissues are rich in new blood vessels, but their structure and function are immature and do not have normal perfusion and delivery functions. The increased permeability of the blood vessel wall causes plasma extravasation, which not only causes local hypoxia and ischemia of the tumor tissue but also leads to the formation of an abnormal tumor microenvironment. All these may aggravate the immune escape and drug resistance of tumors, making it difficult for cytotoxic drugs to be delivered to the deep tumor tissues, thus, reducing therapeutic efficacy.

In this experiment, we first administered HS-173 at a dose of 30 mg/kg to mice that underwent subcutaneous transplantation of tumors for therapeutic research. The results showed that HS-173 inhibited tumor growth and angiogenesis. Further, immunofluorescence and transmission electron microscopy were used to observe the effects of HS-173 on the integrity and continuity of tumor vascular endothelial cells. The results confirmed that compared with the control group, the integrity and continuity of tumor vascular endothelial cells increased after HS-173 treatment, the tumor vascular lumen leaks were reduced, the diameter was uniform, the endothelial cell structure was complete, the morphology was good, and the vascular structures were mature. In addition, after HS-173 treatment, the number of tight junctions between vascular endothelial cells increased, the degree of connection was better, and the formation of the vascular basement membrane was more obvious. These findings indicated that HS-173 could increase the tight junctions of vascular endothelial cells, reduce vascular permeability, and create favorable conditions for the delivery of doxorubicin to deep tumor tissues. Because doxorubicin has its own fluorescence, small animal live imaging can be used to dynamically monitor the delivery of doxorubicin. We monitored the tumor's blood perfusion using Doppler ultrasound. The results showed that after the use of doxorubicin combined with HS-173 treatment, tumor vascular perfusion increased, and the doxorubicin content in tumor tissues was increased. At the same time, compared with the control group and the other two groups alone, the tumor cell apoptosis in the combined drug group was obvious (data not shown), and the tumor growth status was significantly inhibited. Altogether, the combined administration of HS-173 and doxorubicin increased the delivery of doxorubicin and improved its therapeutic effect.

Cell proliferation in tumor tissues is not proportional to the speed of vascular network formation. Therefore, malignant tumor cells often secrete pro-angiogenic factors such as vascular endothelial growth factor VEGF (Vascular Endothelial Growth Factor) to promote angiogenesis. However, the anti-angiogenic factors were not excessively consumed due to the increased secretion of pro-angiogenic factors. The unbalanced secretion of the two angiogenic factors led to disorder in tumor neovascularization, causing a series of metabolic abnormalities in the microenvironment. Therefore, tumor tissue has abundant new blood vessels but immature structure and function, which does not have normal perfusion and delivery functions. The "tumor vascular normalization" theory suggests that proper inhibition of the secretion of pro-angiogenic factors can inhibit tumor angiogenesis and restore the balance of anti-/pro-angiogenic factors, allowing the structure and function of tumor blood vessels to mature [13, 14].

As cell proliferation in tumor tissues is not proportional to the speed of vascular network formation, malignant tumor cells often secrete pro-angiogenic factors such as vascular endothelial growth factor VEGF to stimulate angiogenesis. However, due to the increase in the secretion of pro-angiogenic factors, the anti-angiogenic factors were not over-consumed, resulting in an unbalanced secretion of two angiogenic factors and leading to the structural disorder of tumor neovascularization and a series of metabolic abnormalities in the microenvironment. Therefore, tumor tissue is rich in new blood vessels but immature in structure and function and does not have normal perfusion and delivery functions. The theory of "tumor

blood vessel normalization" suggests that proper inhibition of the secretion of pro-angiogenic factors can inhibit tumor angiogenesis, restore the balance of anti-/pro-angiogenic factors, and allow the structure and function of tumor blood vessels to mature.

The study of vascular normalization targeting VEGF and its receptors has been widely recognized. In a study by Tolaney *et al.* [15], the authors found that inhibiting the expression of VEGF increased pericyte coverage, reduced vascular permeability and matured tumor blood vessels [15, 16]. In addition, studies have shown that VEGFR-2 (Vascular endothelial growth factor receptor 2) inhibitors can increase the tight junctions between endothelial cells and promote vascular maturation [17, 18]. Although the study of VEGF inhibitors has achieved encouraging results, there are still many limitations. For example, anti-VEGF therapy can increase the risk of bleeding or venous thromboembolism, cause severe vascular recessions, and increase the incidence of tumor metastasis [19, 20]. Therefore, people are more inclined to look for alternative targets for the "normalization" of tumor blood vessels, for example, by improving the coverage of pericytes and restoring cell connections to promote blood vessel maturation, thereby increasing tumor perfusion, limiting tumor hypoxia, and improving the effects of antitumor treatment [21–23].

The effects of PI3K on the components of the tumor microenvironment, especially on blood vessels, have attracted increasing attention in recent years. The involvement of PI3K in regulating tumor angiogenesis and inhibiting tumor metastasis has been confirmed in several studies. PI3K inhibitors can reduce the expression of VEGF, which may be one of its mechanisms for promoting the normalization of tumor blood vessels. The PI3K signaling pathway is also necessary for the proliferation of endothelial cells. Soo Jung Kim *et al.* [8] showed that HS-173 could inhibit the sprouting of vascular endothelial cells and maintain the stability of endothelial cells by inhibiting the PI3K/AKT/NOTCH1 (Neurogenic locus notch homolog protein 1) signaling pathway. The effects of PI3K inhibitors on the proliferation and migration of vascular endothelial cells, that is, the direct effect on tumor blood vessels, still require further validation via molecular biology experiments. Based on the above research, we showed that the PI3K inhibitor HS-173 promoted the normalization of tumor vascular structure and function by inhibiting the PI3K/AKT/VEGF signaling pathway in mice models. It also increased the delivery of doxorubicin in tumor tissues, which was associated with an enhancement of the antitumor effects of doxorubicin.

To clarify the effects of PI3Kα subtype inhibitors on tumor angiogenesis, vascular structural integrity and chemotherapy drug delivery function, we used HS-173, a PI3Kα subtype-specific inhibitor, and broad-spectrum chemotherapy drug doxorubicin (DOX) alone or combined treatment in mice. Using small animal ultrasound to monitor the growth of a subcutaneous xenograft model after inoculation with the mouse breast cancer cell line 4T1, HE staining, immunohistochemical staining, immunofluorescence staining and transmission electron microscopy showed that HS-173 inhibited angiogenesis, reduced the tortuosity, swelling and structural disorder of tumor blood vessels, increased the integrity of tumor vascular endothelium, and enhanced endothelial cells tight junctions and basement membrane integrity. Doppler ultrasound and small animal *in vivo* imaging experiments confirmed that HS-173 increased blood perfusion and the delivery of doxorubicin in tumor tissues. In addition, the tumor volume after the combined treatment further proved that HS-173 could enhance the treatment effects of doxorubicin.

In summary, we conclude that HS-173 may inhibit tumor angiogenesis, promote the normalization of tumor vascular structure and function and increase the therapeutic effect of chemotherapy drugs, providing experimental evidence for the normalization of tumor blood vessels.

5. Conclusions

In conclusion, our results demonstrated that PI3K inhibitors increased the integrity of tumor vascular endothelial cells, enhanced endothelial cell-to-cell junctions and basement membrane integrity, increased tumor blood perfusion and the delivery efficiency of doxorubicin, and enhanced the antitumor effect of doxorubicin. Thus, HS-173 may have promising efficacy in inhibiting tumor angiogenesis and improving the structure and function of blood vessels in the tumor microenvironment.

ABBREVIATIONS

DOX: doxorubicin; MVD: microvessel density; PBS: phosphate buffer solution; TGF-β: transforming growth factor-β; VEGF: Vascular Endothelial Growth Factor.

AVAILABILITY OF DATA AND MATERIALS

All data generated or analyzed during this study are included in this published article.

AUTHOR CONTRIBUTIONS

BHL, YYT, HYZ, JZ, JH, LHZ and WL—designed the study. BHL, YYT and HYZ—performed the experiments and acquired the data. JZ, JH, LHZ and WL—provided technical support in performing the experiments. BHL and YYT—confirmed the authenticity of all data; planned all experiments, analyzed and interpreted the data, and drafted the manuscript. All authors are equally responsible for all aspects of the study, including the integrity and accuracy of the data. All authors have read and approved the final manuscript.

ETHICS APPROVAL AND CONSENT TO PARTICIPATE

The study was approved by the Ethics Committee of Experimental Animals, School of Basic Medicine, Jilin University (protocol code 2022.317) and conducted in accordance with the ethical standards. Laboratory animal use license number: SYXK (Ji) 2018-0001.

ACKNOWLEDGMENT

We would like to express gratitude to all those who helped in the performance of this study and in preparation of the manuscript. Thanks to all the peer reviewers for their opinions and suggestions.

FUNDING

The present study was supported by the Fundamental Research Funds for the Central Universities, JLU and the Natural Science Foundation of Jilin Province, China (Grant No. 20170623093-06TC, 20190201091JC).

CONFLICT OF INTEREST

The authors declare no conflict of interest.

REFERENCES

[1] Parmar D, Apte M. Angiopoietin inhibitors: a review on targeting tumor angiogenesis. European Journal of Pharmacology. 2021; 899: 174021.

[2] Haibe Yolla, Kreidieh Malek, El Hajj Hiba, Khalifeh I, Mukherji D, Temraz S, *et al*. Resistance mechanisms to anti-angiogenic therapies in cancer. Frontiers in Oncology. 2020; 10: 221.

[3] Carmen García-Pravia, José A Galván, Natalia Gutiérrez-Corral, Solar-García L, García-Pérez E, García-Ocaña M, *et al.* Overexpression of COL11A1 by cancer-associated fibroblasts: clinical relevance of a stromal marker in pancreatic cancer. PLoS One. 2013; 8: e78327.

[4] Lai Victoria, Neshat Sarah Y, Rakoski Amanda, Pitingolo J, Doloff JC. Drug delivery strategies in maximizing anti-angiogenesis and antitumor immunity. Advanced Drug Delivery Reviews. 2021; 179: 113920.

[5] Kaymak I, Williams KS, Cantor JR, Jones RG. Immunometabolic interplay in the tumor microenvironment. Cancer Cell. 2021; 39: 28–37.

[6] Hui L, Chen Y. Tumor microenvironment: sanctuary of the devil. Cancer Letters. 2015; 368: 7–13.

[7] Sung H, Ferlay J, Siegel RL, Laversanne M, Soerjomataram I, Jemal A, *et al*. Global cancer statistics 2020: GLOBOCAN estimates of incidence and mortality worldwide for 36 cancers in 185 countries. CA: A Cancer Journal for Clinicians. 2021; 71: 209–249.

[8] Kim SJ, Jung KH, Son MK, Park JH, Yan HH, Fang Z, *et al.* Tumor vessel normalization by the PI3K inhibitor HS-173 enhances drug delivery. Cancer Letters. 2017; 403: 339–353.

[9] Zheng R, Li F, Li F, Gong A. Targeting tumor vascularization: promising strategies for vascular normalization. Journal of Cancer Research and Clinical Oncology. 2021; 147: 2489–2505.

[10] Viallard C, Larrivée B. Tumor angiogenesis and vascular normalization: alternative therapeutic targets. Angiogenesis. 2017; 20: 409–426.

[11] Goel S, Duda DG, Xu L, Munn LL, Boucher Y, Fukumura D, *et al*. Normalization of the vasculature for treatment of cancer and other diseases. Physiological Reviews. 2011; 91: 1071–1121.

[12] Feng Y, Deng L, Guo H, Zhao Y, Peng F, Wang G, *et al*. The anti-colon cancer effects of essential oil of *curcuma phaeocaulis* through tumour vessel normalisation. Frontiers in Oncology. 2021; 11: 728464.

[13] Erskine L, François U, Denti L, Joyce A, Tillo M, Bruce F, *et al*. VEGF-A and neuropilin 1 (NRP1) shape axon projections in the developing CNS *via* dual roles in neurons and blood vessels. Development. 2017; 144: 2504–2516.

[14] Jia JD, Jiang WG, Luo X, Li RR, Zhao YC, Tian G, *et al.* Vascular endothelial growth factor B inhibits insulin secretion in MIN6 cells and reduces $Ca2^{+}$ and cyclic adenosine monophosphate levels through PI3K/AKT pathway. World Journal of Diabetes. 2021; 12: 480–498.

[15] Tolaney SM, Boucher Y, Duda DG, Martin JD, Seano G, Ancukiewicz M, *et al*. Role of vascular density and normalization in response to neoadjuvant bevacizumab and chemotherapy in breast cancer patients. Proceedings of the National Academy of Sciences. 2015; 112: 14325–14330.

[16] Krüger K, Silwal-Pandit L, Wik E, Straume O, Stefansson IM, Borgen E, *et al.* Baseline microvessel density predicts response to neoadjuvant bevacizumab treatment of locally advanced breast cancer. Scientific Reports. 2021; 11: 3388.

[17] Makhoul I, Griffin RJ, Siegel E, Lee J, Dhakal I, Raj V, *et al*. High-circulating Tie2 is Associated with pathologic complete response to chemotherapy and antiangiogenic therapy in breast cancer. American Journal of Clinical Oncology. 2016; 39: 248–254.

[18] Harry JA, Ormiston ML. Novel pathways for targeting tumor angiogenesis in metastatic breast cancer. Frontiers in Oncology. 2021; 11: 772305.

[19] Zhu D, Li Y, Zhang Z, Xue Z, Hua Z, Luo X, *et al*. Recent advances of nanotechnology-based tumor vessel-targeting strategies. Journal of Nanobiotechnology. 2021; 19: 435.

[20] Hultgren NW, Fang JS, Ziegler ME, Ramirez RN, Phan DTT, Hatch MMS, *et al.* Slug regulates the Dll4-Notch-VEGFR2 axis to control endothelial cell activation and angiogenesis. Nature Communications. 2020; 11: 5400.

[21] Zhang Q, Lu S, Li T, Yu L, Zhang Y, Zeng H, *et al*. ACE2 inhibits breast cancer angiogenesis via suppressing the VEGFa/VEGFR2/ERK pathway. Journal of Experimental & Clinical Cancer Research. 2019; 38: 173.

[22] Shah AA, Kamal MA, Akhtar S. Tumor angiogenesis and VEGFR-2: mechanism, pathways and current biological therapeutic interventions. Current Drug Metabolism. 2021; 22: 50–59.

[23] Benedito R, Rocha SF, Woeste M, Zamykal M, Radtke F, Casanovas O, *et al*. Notch-dependent VEGFR3 upregulation allows angiogenesis without VEGF–VEGFR2 signalling. Nature. 2012; 484: 110–114.

How to cite this article: Baihui Li, Yuanyuan Tian, Ju Huang, Haiying Zhang, Jiao Zhao, Lihong Zhang, *et al*. PI3K inhibitor promotes tumor vessel normalization and improves treatment outcomes of breast cancer with doxorubicin. European Journal of Gynaecological Oncology. 2023; 44(4): 55-65. doi: 10.22514/ejgo.2023.058.